**SINERGI** Vol. 29, No. 2, June 2025: 347-360
http://publikasi.mercubuana.ac.id/index.php/sinergi
http://doi.org/10.22441/sinergi.2025.2.007

# Evaluation of FIR bandpass filter and Welch method implementation for centrifugal pump fault detection

**Dedik Romahadi[1,2,*], Aberham Genetu Feleke[2], Tri Wahyu Adinarto[1], Dafit Feriyanto[1], Agung Wahyudi Biantoro[1], Fatkur Rachmanu[3]**
[1]Department of Mechanical Engineering, Faculty of Engineering, Universitas Mercu Buana, Indonesia
[2]School of Mechanical Engineering, Beijing Institute of Technology, China
[3]Manufacture Engineering Technology, Politeknik Enjinering Indorama, Indonesia

***Abstract***
*The motivation for this research is the high vibration observed during the operation of the centrifugal cooling water pump. Our study aims to assess the pump's state and check the vibrations to ensure the factors underlying the fault of the centrifugal pump in the alkaline chlorine factory. While previous studies have primarily used spectral amplitude results from the Fast Fourier Transform to analyze engine vibrations, we propose a different approach in this study. We employ the Finite Impulse Response (FIR) Bandpass Filter and the Welch Method, a practical analytic approach. The ISO 10816-3 standard is a benchmark of the RMS value to determine the pump's condition. The FIR Bandpass Filter and Welch Method prove to be highly effective in describing and modifying the vibrational signals of the centrifugal pump. The approach is particularly beneficial as it is consistent across sample rate settings, reduces the vibration of amplitude low, produces a smoother spectrum with only the primary frequency component, and segments the vibration signal into the frequency band-aids to identify the primary vibration source. The diagnostic results reveal increased vibrations at 1x, 2x, and ball pass frequency (BPF), indicating impeller damage and disappearance. Post-repair, the vibration value experiences a significant drop, as per the fault analysis results, further confirming the high effectiveness of our approach. These findings have practical implications for the maintenance and fault diagnosis of centrifugal pumps, providing a reliable and effective method for identifying and addressing issues.*



***Keywords:***
*FIR bandpass filter;*
*Machine fault analysis;*
*Vibration analysis;*
*Welch method;*

***Article History:***
*Received: July 3, 2024*
*Revised: September 14, 2024*
*Accepted: September 26, 2024*
*Published: May 1, 2025*

***Corresponding Author:***
*Dedik Romahadi*
*Mechanical Engineering Department, Universitas Mercu Buana, Indonesia*
*School of Mechanical Engineering, Beijing Institute of Technology, China*
*Email:*
*dedik.romahadi@mercubuana.ac.id*

## INTRODUCTION

The centrifugal pump moves liquid from one location to another by strengthening fluid pressure [1, 2, 3]. This kind of pump is a centrifugal pump specifically designed for water cooling in the heat exchanger system. During operation in the field, the centrifugal pump experienced a reasonably large vibration. Failure to overcome excessive vibrations can cause severe damage to the pump. Predictive maintenance requires using condition-monitoring techniques, especially those related to machine vibrations, to carry out practical maintenance tasks [4, 5, 6, 7].

Machine vibration is usually caused by wear or structural damage, such as bearing problems, abnormal vibration, and cavitation. Abnormal vibrations can also be caused by mechanical leeway, which refers to the reduction in bolt firmness or other binding systems [8, 9, 10]. Cavitation is a phenomenon that occurs when the pressure in the liquid drops to the level under pressure, resulting in the formation of bubbles [11]. These bubbles have the potential to cause damage to various components and cause irregular vibrations.

Nicusor et al. [12] and Bhaumik et al. [13] conducted a case study of machines that showed significant vibrations in previous studies. Their research aims to determine the nature of the damage experienced by the machine through the use of fast Fourier transform (FFT) techniques. FFT is a conventional technique used to change vibrations in the form of time domain into domain frequency [14, 15, 16, 17]. Their investigation findings of vibration spectrum analysis show that the gearbox motor shows imbalance and damage to the bearing due to excessive vibration. This is evidenced by the presence of 1x, 2x, and frequency of bearing frequencies. The study by Lian et al. [18] involved a numerical model to evaluate the amount of solid and liquid object vibrations in the tunnel. Research from Taghipour et al. [19] aims to analyze the ratio of mass loading experienced by the Rotor. Experimental findings show that imbalance and misalignment significantly impact the vibration level, as evidenced by a 1x and 2x work cycle. In addition, it was observed that the amount of vibration increased with the burden of imbalance applied to the rotor.

Power spectral densities (PSD) quantify and compare various vibration conditions obtained from Welch's method [20], [21]. The PSDs are standardized to the frequency bin width, ensuring that the duration of the data set and the associated frequency step do not affect the amplitude of the outcome [22]. FFT does not perform this function. The problem is that centrifugal pump vibration measurements sometimes use different instrument settings. PSDs are favored over FFTs for vibration analysis due to their normalization to bin width. This enables the comparison of PSDs across different contexts, testing instrumentation, settings, and duration, ensuring a consistent comparison. Ahmadi et al. [23] computed the RMS and PSD of an electromotor under various fault conditions. The results indicated that calculating the PSD may promptly identify faults and diagnose the electromotor. It was demonstrated by Tang et al. [24] A defect detection method was employed to extract inherent state functions continuously using PSD.

This study aims to evaluate the implementation of the FIR bandpass filter and PSD derived from the Welch method to identify primary frequencies in the centrifugal pump responsible for excessive vibrations observed in the frequency domain. In contrast to previous research efforts, which obtain spectral amplitude by applying the FFT, this study includes these methods and evaluates the results of both methods. FIR bandpass filter and the Welch approach are two strategies used in vibration spectrum analysis. Measuring devices known as Vibxpert II are used to take measurements. This instrument uses three different measurement directions: horizontal, vertical, and axial. The RMS algorithm processes all vibration data, and the results are compared with ISO 10816-3 standards. Welch algorithms are used to conduct fault analysis that occurs in centrifugal pumps through the use of frequency domain computing.

## MATERIAL AND METHOD

### Vibration Measurement

This study uses Vibxpert II measurement devices to measure pump vibrations. Figure 1 illustrates the instruments used for vibrational data acquisition. Table 1 shows the specifications of the Vibxpert II vibration measuring device, while Table 2 shows the specifications of the VIB accelerometer sensor, 6.142.

In this study, we used a cooling water centrifugal pump, as shown in Figure 2, an essential component of the cooling tower system, in this investigation. The power possessed by the centrifugal pump with a shaft rotation of 1450 rpm is 114.4 kW. The fluid is channeled from a cooling tower to a heat exchanger through the centrifugal pump at PT SAU.


Figure 1. VibXpert II

Table 1. VibXpert II Specification

| NAME | SPECIFICATION |
|---|---|
| Range Frequency | 0.5 Hz – 40 kHz |
| Environment Protection | IP65 |
| Temperature Operational | $0^0$C to $50^0$C |
| Memory | 128 MB DDR RAM |
| Battery Type | Li-Ion *rechargeable* (7.3V / 5.3Ah – 38.7Wh) |
| Dimension | 186 x 162 x52 mm (LxWxH) |

Table 2. Vib. 6.142 Specification

| NAME | SPECIFICATION |
|---|---|
| Transmision Factor | 1,0 µA/m/s$^2$ |
| Resonance Frequency | 36 kHz |
| Temperature Range | -40$^0$C to 100$^0$C |
| Case Material | Stainless steel VA 1.4305 |
| Environment Protection | IP 65 |


Figure 2. Centrifugal Water Pump

Table 3. Centrifugal Pump P9114B Specification

| NAME | SPECIFICATION |
|---|---|
| Pump Type | Centrifugal Pump |
| Model | 3K 10 X 8-16/156 |
| Brand | DURCO MARK III |
| Suction Press | 5.5 Bar |
| RPM | 1450 |
| Power | 114.4 Kw |

The bearing type used on the P9114B drive end (DE) pump is the 3314-type angular contact bearing, while on the (non-drive end) NDE and DE-NDE motor side is the ball cushion in the 6314-type groove. The gland packing type is used to seal asbestos, other than lubricating lubricants. The centrifugal cooling water pump specifications are shown in Table 3.

## Machine Component Frequency

Frequency specifications and calculations are vital in machine fault analysis, especially at bearing frequencies. The pump uses type 6314 ball bearings and has detailed specifications, as shown in Table 4. Bearing characteristic frequencies, such as inner and outer race, ball or roller, and cage frequencies, are shown in (1)-(4). If a bearing element frequency is proven, it indicates a bearing defect related to pump damage [25].

$$BPFI = \frac{RPM}{120}\left(1+\frac{D_B}{D_P}\cos\beta\right) \tag{1}$$

$$BPFO = \frac{RPM}{120}\left(1+\frac{D_B}{D_P}\cos\beta\right)\cdot N_B \tag{2}$$

$$BSF = \frac{RPM}{120}\left(1-\left(\frac{D_B}{D_P}\cos\beta\right)^2\right)\cdot\frac{D_P}{D_B} \tag{3}$$

$$FTF = \frac{RPM}{120}\left(1-\frac{D_B}{D_P}\cos\beta\right) \tag{4}$$

Where:

| | | |
|---|---|---|
| FTF | : | Fundamental Train Frequency |
| BPFI | : | Ball Pass Frequency of Inner Ring |
| BPFO | : | Ball Pass Frequency of Outer Ring |
| BSF | : | Ball Spin Frequency |

The pump impeller has 6 blade angles. The pump shaft rotates at 1450 RPM or 24.17 Hz. Use (5) to calculate the frequency produced by the pump impeller.

$$BPF = \frac{B_N}{60}\times RPM \tag{5}$$

$B_N$ is the number of blades, and RPM is the shaft rotation in Hz.

## Vibration Signal Processing

Vibration measurements were carried out to collect centrifugal pump vibration data. The data was collected using the VibXpert II tool at both inboard and outboard sites. Measurements were carried out in three directions, namely horizontal, vertical, and axial, both on the motor and pump sides. The data processing technique was then carried out using MATLAB software. Vibration data in the time domain is derived using the RMS technique for vibration, as stated in (6) [26].

$$x_{RMS} = \sqrt{\frac{1}{N}\sum_{i=1}^{N} x_i^2} \tag{6}$$

Where:

| | | |
|---|---|---|
| $x_{RMS}$ | : | Root means square value |
| $N$ | : | Number of values |
| $x_i$ | : | Each value in the dataset |

The RMS calculation results compared with the ISO 10816-3 standard. This aims to determine the level and condition of pump vibration. ISO 10816, as shown in [27], provides criteria for assessing vibration levels when measured directly at the measurement location [28]. The specified criteria apply to machine devices with power above 15 kW and an operating speed between 120 and 15000 RPM.

Table 4. Centrifugal Bearing Frequency

| NAME | SPECIFICATION |
|---|---|
| RPM | 1450 (24.17 Hz) |
| Pitch Diameter ($D_P$) | 100 mm |
| Outside Diameter ($D_O$) | 150 mm |
| Inside Diameter ($D_I$) | 70 mm |
| Number of Balls ($N_B$) | 8 |
| Ball Diameter ($D_B$) | 20 mm |
| Contact Angle (β) | 0° |

The ISO 10816-3:2009 velocity type standard assesses vibration in machines with a more than 600 RPM rotational speed. Generally, vibration assessment uses mm/s RMS units. If the RMS value is lower than the limit in the ISO 10816-3 group 2 standard with a rigid foundation type, i.e., 2.8 mm/s, then the pump vibration value is still good, so there is no need to proceed to the following procedure. On the other hand, if the vibration exceeds 2.8 mm/s, then analysis to find the source of the damage needs to be carried out.

The initial stage to find the source of damage is to apply the bandpass finite impulse response (FIR) algorithm to select the frequency with the highest energy [29], as shown in (7)-(13).

$$h_{ideal}(n) = h_{ideal,high}(n) - h_{ideal,low}(n) \tag{7}$$

The impulse response $h_{ideal}(n)$ of the perfect bandpass filter is obtained by subtracting the impulse responses of two ideal low-pass filters, where,

$$h_{ideal,low}(n) = \frac{sin\left(\frac{2\pi f_{low}}{fs}\left(n-\frac{N}{2}\right)\right)}{\pi(n-\frac{N}{2})} \tag{8}$$

$$h_{ideal,high}(n) = \frac{sin\left(\frac{2\pi f_{high}}{fs}\left(n-\frac{N}{2}\right)\right)}{\pi(n-\frac{N}{2})} \tag{9}$$

for $n = N/2$:

$$h_{ideal,low} N/2 = \frac{\omega_{low}}{\pi} \tag{10}$$

$$h_{ideal,high} N/2 = \frac{\omega_{high}}{\pi} \tag{11}$$

Where:

| | | |
|---|---|---|
| $h(n)$ | : | Impulse response of the FIR filter (filter coefficients) |
| $N$ | : | Number of filter taps (order of the filter + 1) |
| $f_{low}$ | : | lower cutoff frequency (normalized by the sampling frequency) |
| $f_{high}$ | : | upper cutoff frequency |
| $\omega(n)$ | | chosen window function |

The Hanning window function, denoted as $w(n)$, regulates the oscillation in both the passband and stopband. Convolve the ideal impulse response with this window to obtain the final impulse response, as depicted in (12).

$$h(n) = h_{ideal}(n) \cdot w(n) \tag{12}$$

Where $w(n)$is defined for n = 0, 1, 2, 3, …, N. The ultimate filter coefficients $h(n)$ are computed for n=0, 1, 2, ..., N.

A vibration signal exhibiting frequency clustering was acquired after successfully implementing FIR bandpass filtering. Subsequently, the Welch method was employed to process the signal and derive its power spectral density (PSD). All spectrum analysis procedures include converting the time-domain representation of a vibration signal into a frequency-domain representation. An analysis of the relative amounts of vibration in different frequency ranges can often provide valuable information on the nature of the resulting damage. To analyze a continuous signal across time, it is necessary to determine the PSD for the stationary process. This pertains to the power distribution in the signal or time series across different frequencies. In this context, power refers to tangible physical force or, more commonly, it is used to describe the magnitude of abstract signals, represented by the square of the signal's value. Equation 13 is the primary formula for calculating the Welch PSD estimate [30][31].

$$\hat{S}(f) = \frac{1}{LM}\sum_{m=0}^{M-1}\left|\sum_{n=0}^{L-1} x_m[n]\omega[n]e^{-j2\pi fn/L}\right|^2 \tag{13}$$

Where:

| | | |
|---|---|---|
| $\hat{S}(f)$ | : | Welch PSD at frequency $f$ |
| $x_m[n]$ | : | The m-th segment of the signal (with length $L$) |
| $M$ | : | number of segments |
| $\omega[n]$ | : | window function applied to each segment |
| $L$ | : | Length of each segment |
| $f$ | : | The frequency at which the PSD is estimated |

The term inside the summation computes the squared magnitude of the DFT of the m-th segment, which is averaged over all segments. PSD can be extended to finite time series with amplitude 1≤*n*≤*N*, such as signals sampled at discrete periods $x_n = x(n\Delta t)$, over a total measurement duration $T = N\Delta t$. Adjacent segments overlap by 50%. Then, average the power spectrum across all segments to produce the final PSD estimate.

## RESULTS AND DISCUSSION

### Machine Component Frequency

Vibrations are generated at varying frequencies by different sources of vibration. By examining individual frequencies within the vibration signal, we can determine the origin of the vibration, be it due to imbalance, misalignment, mechanical instability, bearing abnormalities, gear malfunctions, or other issues. Gaining insight into the frequency components of vibration aids in the precise identification of problems. For instance, if a specific frequency aligns with a particular component or the rotational speed of a machine, this can direct the technician to concentrate the examination for that particular location, leading to a more effective diagnosis and troubleshooting process. Table 5 displays the frequency of components in centrifugal pump machines.

### Vibration Measurement Results

Changes in vibration amplitude in centrifugal cooling pump machines can indicate a fault or abnormality. Based on the ISO 10816 standard, an amplitude increases exceeding 2.8 mm/s may indicate wear, misalignment, imbalance, or other mechanical problems. Monitoring the amplitude over time will help in predictive maintenance, allowing timely intervention before a major failure occurs in the machine.

Table 6 and Table 7 show that the amplitudes are used to assess machine conditions. Table 6 shows the overall RMS value for the motor part before repairs occur. Regarding the ISO 10816-3 standard, almost all vibrations in motor parts are still in the good category. Only one vibration originating in the horizontal axis DE bearing falls into the permitted short-term operation category. Table 7 shows the overall RMS vibration on the pump side. In contrast to the motor section, the vibrations on the pump side are more significant. According to ISO standards, many vibrations fall into the short-term operation category, and one value falls into the vibration category that can cause damage; in other words, the machine must be repaired immediately.

Table 5. Frequency Components

| Frequency Components | Frequency (Hz) |
|---|---|
| BPFI | 118.98 |
| BPFO | 74.34 |
| BSF | 38.67 |
| FTF | 9.29 |
| BPF | 148.5 |

Table 6. Overall Motor Vibration Before Repair

| Date | NDE V (mm/s) | NDE H (mm/s) | DE V (mm/s) | DE H (mm/s) | DE A (mm/s) |
|---|---|---|---|---|---|
| 18/01 | 0.92 | 1.17 | 1.41 | 1.75 | 0.90 |
| 25/01 | 1.04 | 1.34 | 1.51 | 1.72 | 1.06 |
| 01/02 | 1.73 | 1.99 | 1.56 | 2.25 | 1.05 |
| 08/02 | 1.53 | 1.91 | 1.46 | 2.38 | 1.01 |
| 15/02 | 1.72 | 1.89 | 1.62 | 2.08 | 1.36 |
| 22/02 | 1.81 | 2.02 | 1.59 | 2.28 | 1.35 |
| 02/03 | 1.93 | 2.00 | 1.57 | 2.30 | 1.35 |
| 09/03 | 2.00 | 2.40 | 2.00 | 3.00 | 1.70 |

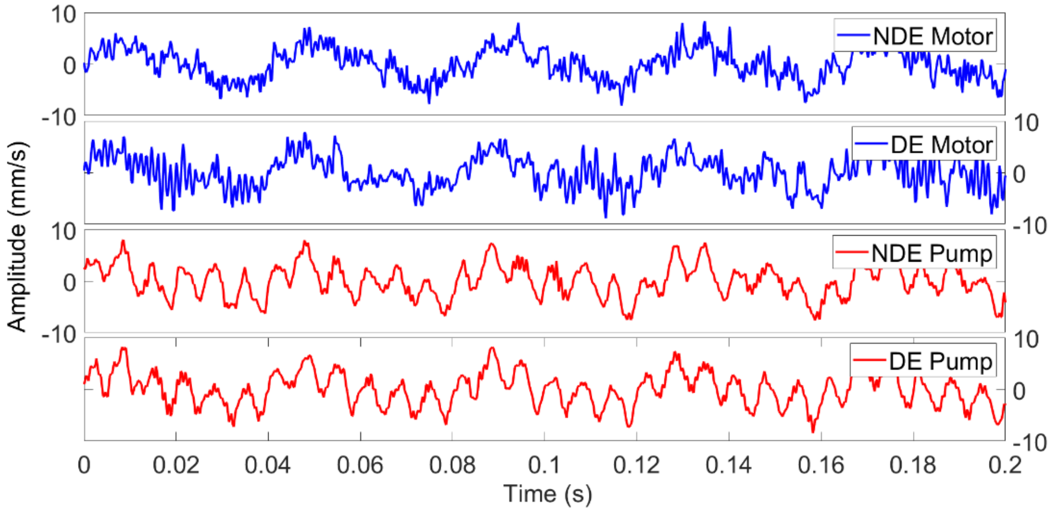


Figure 3. Time Domain Vibration

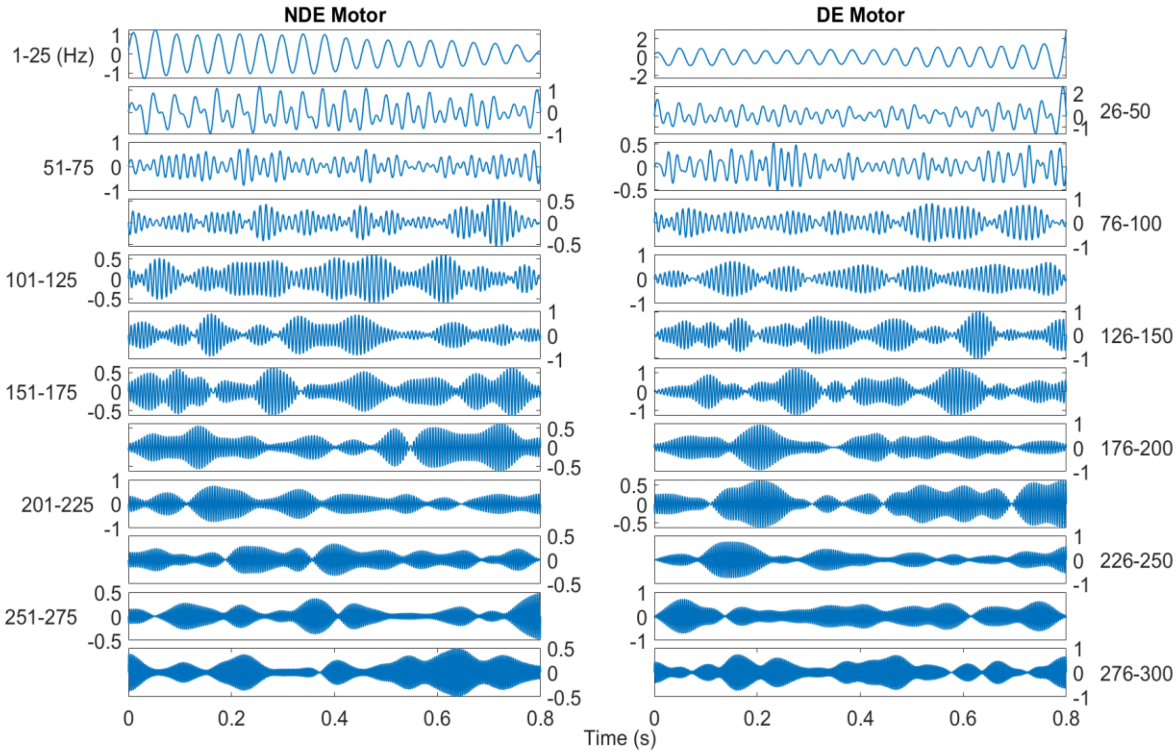


Figure 4. Motor Vibration Decomposition

Establishing and operating a condition-monitoring program becomes possible by continuously monitoring vibration data over a while. By setting initial vibration patterns and monitoring departures from these patterns, as seen in Figure 3, we may anticipate possible malfunctions and plan maintenance tasks. This approach helps to minimize periods of inactivity and decrease expenses related to maintenance. We choose a single set of vibration data from each location point on the horizontal axis of the machine's measurement. The blue vibration signal represents measurements from the motor component, while the red hue corresponds to the pump. According to the graph, the pump exhibits prominent vibrations at low frequencies, whereas the motor is predominantly affected by high frequencies. To identify the primary vibration source in the machine, we employ FIR bandpass filtering to separate the vibrations into distinct frequency groups. This process is illustrated in Figure 3, and the resulting 12 frequency groups can be observed in Figure 4 and Figure 5.

These figures show the vibration signal after decomposing by the FIR bandpass filter algorithm. Regarding the amplitude value, at the y-axis, there are high vibrations in the low-frequency band compared to other bands, namely 1 – 25 Hz and 26 – 50 Hz at both motor vibration measurement points. The same thing can also be seen in pump vibrations, as shown in Figure 10. The highest amplitude is at low frequencies. The frequency that arises is closely related to the fundamental motor rotation, 24.17 Hz. To diagnose the source of vibration triggers more clearly in the centrifugal pump, we transformed it into a spectrum using the FFT and Welch methods. Spectrum is a vibration displayed in the frequency domain. In contrast to FFT, the Welch method normalizes the amplitude to a single hertz bandwidth. The results of the Welch method transformation can be seen in Figure 6 and Figure 7.

Table 7. Overall Pump Vibration Before Repair

| Date | DE V (mm/s) | DE H (mm/s) | NDE V (mm/s) | NDE H (mm/s) | NDE A (mm/s) |
|---|---|---|---|---|---|
| 18/01/2023 | 2.23 | 2.86 | 2.38 | 2.55 | 2.3 |
| 25/01/2023 | 2.99 | 2.89 | 2.47 | 2.65 | 2.3 |
| 01/02/2023 | 2.74 | 3.3 | 2.57 | 3 | 2.33 |
| 08/02/2023 | 2.69 | 3.4 | 2.5 | 3.08 | 2.3 |
| 15/02/2023 | 2.67 | 3.89 | 2.72 | 3.4 | 2.31 |
| 22/02/2023 | 2.65 | 3.9 | 2.86 | 3.3 | 2.2 |
| 02/03/2023 | 2.73 | 4 | 2.89 | 3.23 | 2.35 |
| 09/03/2023 | 3 | 5.16 | 3.66 | 3.66 | 2.7 |

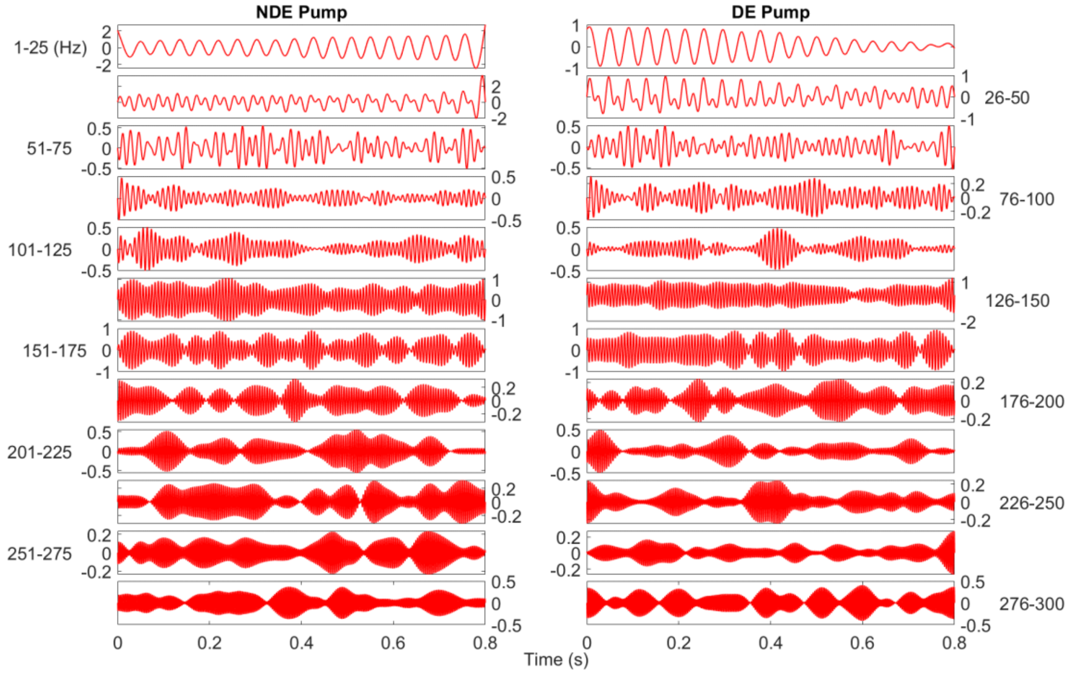


Figure 5. Pump Vibration Decomposition

Figure 6 displays vibrations in the frequency domain characterized using an FIR bandpass filter. Signals positioned around the intersection point of the frequency window can still be observed in the filtering results window during the signal decomposition process and observed through the window located in the leftmost column of the second row. Two amplitudes arise from the primary rotation of the motor, occurring twice, despite implementing an FIR bandpass filter within the frequency range of 26 – 50 Hz. The presence of two amplitudes at frequencies 1X and 2X suggests a misalignment in the machine shaft. The traits mentioned earlier are also evident in Figure 7 within the identical frequency range. Based on the information provided by the two vibration graphs, we can tentatively infer that the primary vibration sources are found within the frequency ranges of 1-25, 26-50, and 51-75. To verify the prevailing vibrations in the machine, we aggregate the vibrations from each window into signal energy. We calculate the quotient of each average value on one window and all windows. Figure 8 displays the outcomes of the accumulated signal energy.

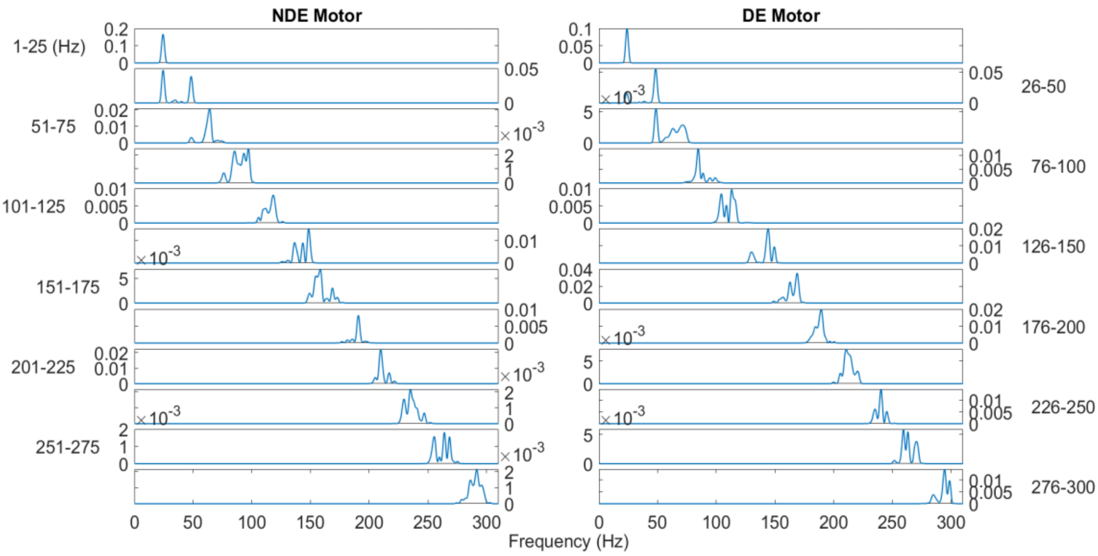


Figure 6. Frequency Domain in Decomposed Motor Vibration

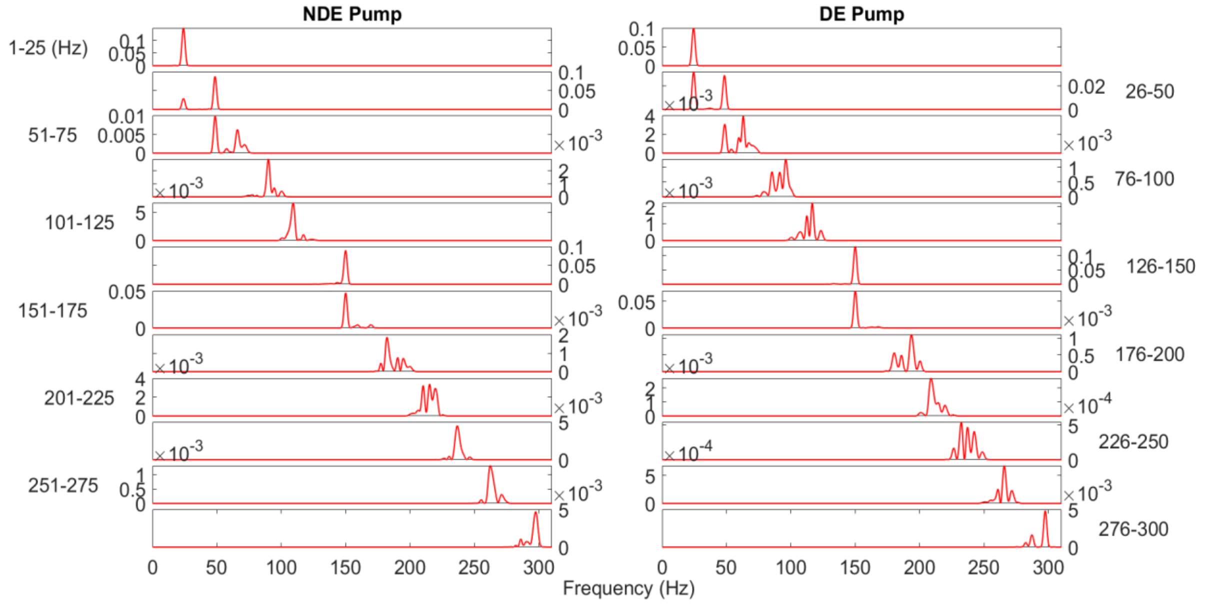


Figure 7. Frequency Domain in Decomposed Pump Vibration

Figure 8 shows that the most potent vibration comes from the pump's NDE bearing, i.e., at 1-25 Hz, accounting for 40% of the overall vibration. The second most prevalent vibration occurs in the DE pump at a frequency range of 126-150 Hz. The subsequent most prevalent vibrations occur within 26 - 50 Hz and 176 - 200 Hz. Utilizing a signal energy graph obtained by averaging the energy of a particular frequency window across all windows facilitates the identification of the origin of present vibrations. Using signal energy, we may bypass the need to analyze each frequency included in a comprehensive frequency, including all machine component vibrations. Instead, we can instantly pinpoint the specific location of the most prominent vibration. By examining our energy signal graph, we can directly investigate all measurement locations and identify components that exhibit significant vibrations. Once the location of the dominating vibrations in the machine is determined, the Welch method may be applied to analyze the vibrations in the entire time domain. Furthermore, we offer the transformation outcomes of the fast Fourier approach to compare the results obtained from both methods.

### Comparison of Welch and FFT

Figure 9 and Figure 10 show the results of the FFT and Welch transformation. In this research, the FFT and Welch methods convert vibrations in the time domain into the frequency domain. This allows us to analyze the frequency components in vibrations in centrifugal pumps.

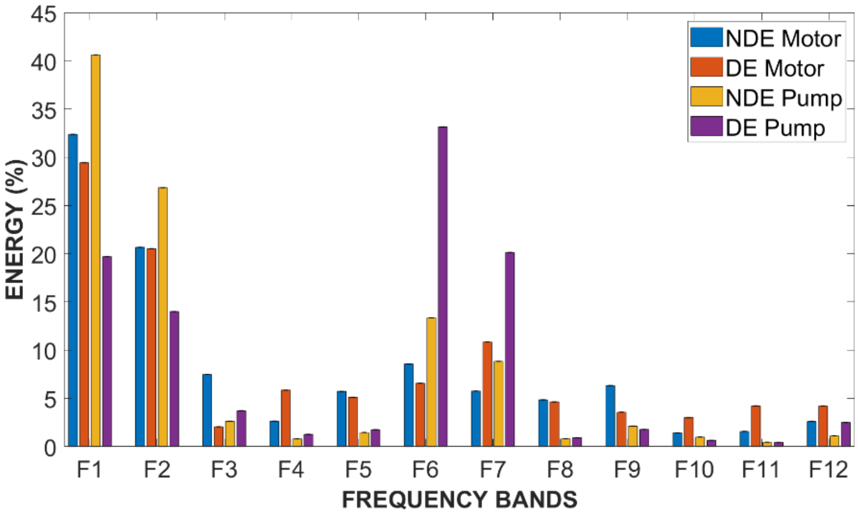


Figure 8. Energy Bands Before Repair

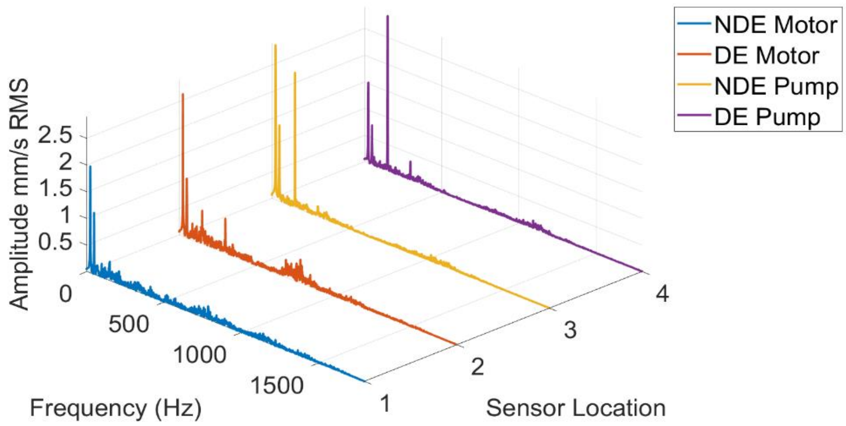


Figure 9. Spectrum Produced by FFT

The Welch method is more widely used to estimate spectral density, especially when dealing with power spectra that vary over time. Simply put, the FFT is primarily employed to convert signals from the time domain to the frequency domain. On the other hand, the Welch method is used in this context to estimate the power spectrum density of vibrations. This results in a smoother spectrum by eliminating vibrations caused by noise or small amplitude high-frequency components. Our primary objective is to address core engine issues such as unbalance, misalignment, impeller damage, and foundation concerns

The spectrum of the FFT computation results is depicted in Figure 9. By employing the FFT, it is observed that a more significant number of low amplitudes are disregarded compared to utilizing the Welch approach, as depicted in Figure 10. The Welch approach involves applying a Hann window to the intact signal, resulting in a signal cut of 50%. In addition, the Welch computation involved windows that overlapped by 25%. The spectrum obtained by the Welch approach exhibits a smoother appearance, with only the most prominent vibration components present. Both signals have identical frequency components when considering the primary signal energy depicted in Figure 8. To enhance the visibility of the primary vibrations in the spectrum generated by the FFT and Welch's method, we specifically concentrated on frequencies ranging from 0 to 300 Hz, as depicted in Figure 11 and Figure 12. Both methods can show the dominant frequency source of the centrifugal pump. If we compare the two graphs, the FFT method, shown in Figure 11, is more sensitive to tiny vibrations than the Welch method, shown in Figure 12. In damage analysis, tiny vibrations that can lead to noise are usually ignored to facilitate the analysis.

In reviewing the method's reliability in overcoming variations in vibration-measuring instrument settings in an industry. We varied the frequency samples by five from the number of primary frequency samples of 4090. It can be seen that the computational results using FFT can significantly affect the vibration amplitude value. Figure 11 shows that the greater the frequency of samples, the greater the amplitude on the spectrum. Similar study results were also shown by previous research [14], [16].

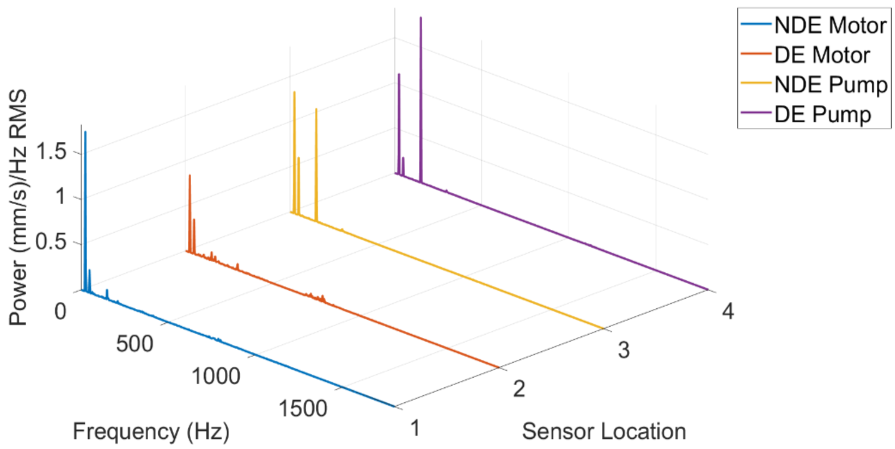


Figure 10. PSD Produced by Welch

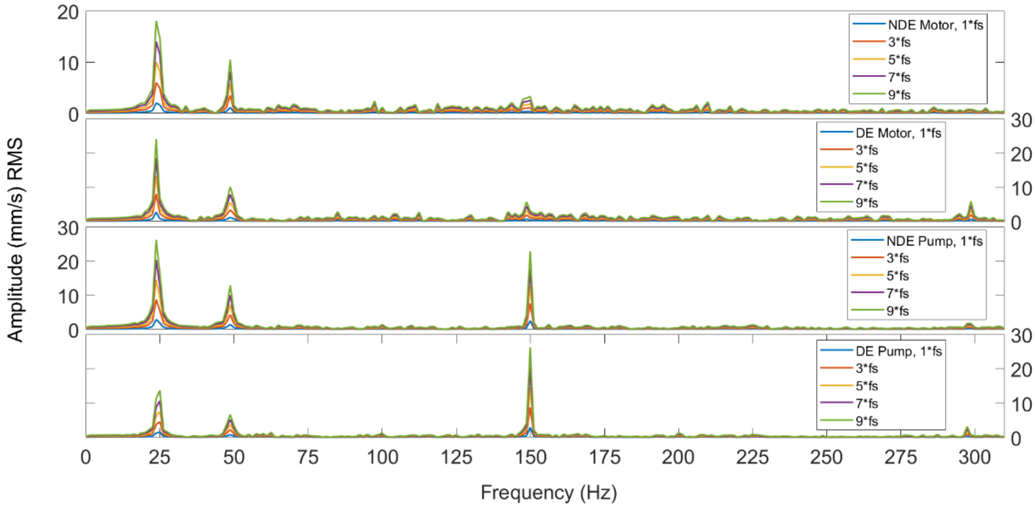

Figure 11. Comparison of Frequency Samples to FFT Results

However, the amplitude level does not affect pattern recognition, which is commonly used for developing classification models [14, 15, 32]. In other cases, this can cause misunderstandings for staff who perform vibration analysis, sometimes when measuring one machine using a different number of samples at each measurement point. Significant differences in amplitudes produced by the FFT can be misinterpreted as the level of damage, in contrast to the results of PSD computation using the Welch method. The amplitude value is not at all affected by the number of frequency samples used. Referring to the differences in the results of the two methods, we recommend using the Welch method for frequency domain analysis.

Figure 12 displays the spectrum obtained using the Welch approach, specifically focusing on frequencies ranging from 0 to 300 Hz. The primary vibrations in the centrifugal pump are observed at 1X, 2X, and 6X, forming the BPF. The signal energy graph demonstrates identical outcomes. Based on Charlotte's vibration analysis reference, vibrations at 1 and 2 fundamental engine revolutions suggest a misalignment issue with the engine shaft [19]. Hence, based on the findings of this research, realigning the shaft both angularly and parallelly is advised. Furthermore, examining and cleaning the channels and impeller concerning the presence of 6X or BPF frequencies is necessary.

Repairs were made based on the vibration analysis of the centrifugal pump. When checked, the condition of the impeller blade was damaged and had holes, as shown in Figure 13(a). In other parts, the impeller surface was also eroded. With the condition of the impeller like this, a new impeller was replaced. The replacement was carried out on the H-type rubber clutch part, which was already worn out, so it did not meet the clutch precisely, as seen in Figure 13(b). They were still in good condition for other components, so there were no repairs or replacements.

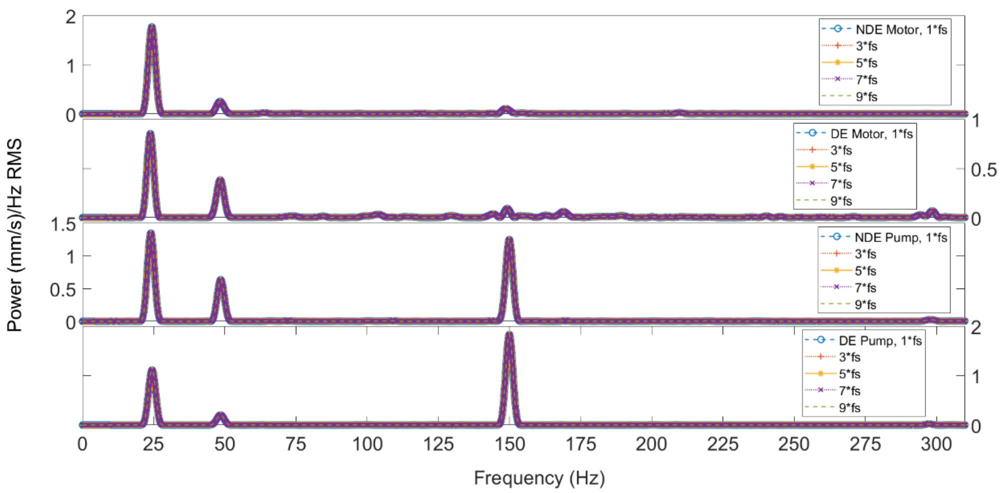

Figure 12. Comparison of Frequency Samples to Welch Results


(a) (b)

Figure 13. Impeller (a) and H-type Rubber Clutch (b) Conditions

## Measurement Results After Repair

Enhancements were implemented based on the results of the centrifugal pump vibration analysis. Upon inspection, it was observed that the impeller blade was damaged and had a hole. Additionally, worn-down impeller surfaces were discovered in other areas. Given the impeller's current state, replacing it with a new one is necessary. The rubber component of the H-type clutch was substituted due to wear, resulting in an imprecise fit with the clutch. The remaining elements are in satisfactory condition; hence, no repairs or replacements are necessary. Figure 14 illustrates the signal's energy following enhancements to the centrifugal pump. The energy signal at each frequency indicates that the primary oscillation in the centrifugal pump occurs within the frequency range of 1 to 25 Hz. The percentage depicted in this graph does not indicate the machine's vibration magnitude. The vibration magnitude inspection must consider the entire root mean square (RMS) value of vibration. The post-repair vibration values are displayed in Table 8. The modifications resulted in a substantial decrease in vibrations on the motor parts, as shown in Table 8. We conducted four iterations of measurements to confirm the accuracy and precision of the measurement data. All vibrations decrease at every measuring location. Figure 15 and Figure 16 visualize vibration in both the time and frequency domains.

Both figures demonstrate that vibrations resulting from misalignment and BPF are minimal. There is a significant disparity between the spectrum before and after improvement. These results validate all values for the overall RMS vibration on both the motor and pump side, in addition to confirming the findings of the vibration analysis conducted and the successful application of the Welch method to centrifugal pump fault analysis. Undeniably, the FFT method is more widely used than the Welch method because the FFT computation time is faster and better for clean and stationary signals [33]. However, this Welch method approach can be relied on when dealing with noise, changing signals, and uncertain measurement parameters [34, 35, 36].

Table 8. Overall Vibration After Repair

| PART | NDE V (mm/s) | NDE H (mm/s) | DE V (mm/s) | DE H (mm/s) | DE A (mm/s) |
|---|---|---|---|---|---|
| **Motor** | 0.67 | 0.65 | 1.23 | 1.48 | 0.93 |
| **Pump** | 1.42 | 1.78 | 1.41 | 1.51 | 0.98 |

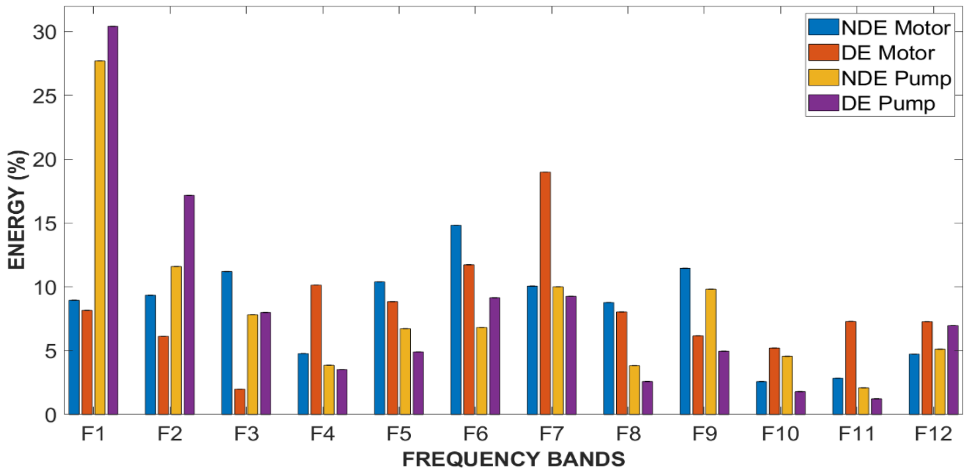


Figure 14. Energy Bands After Repair

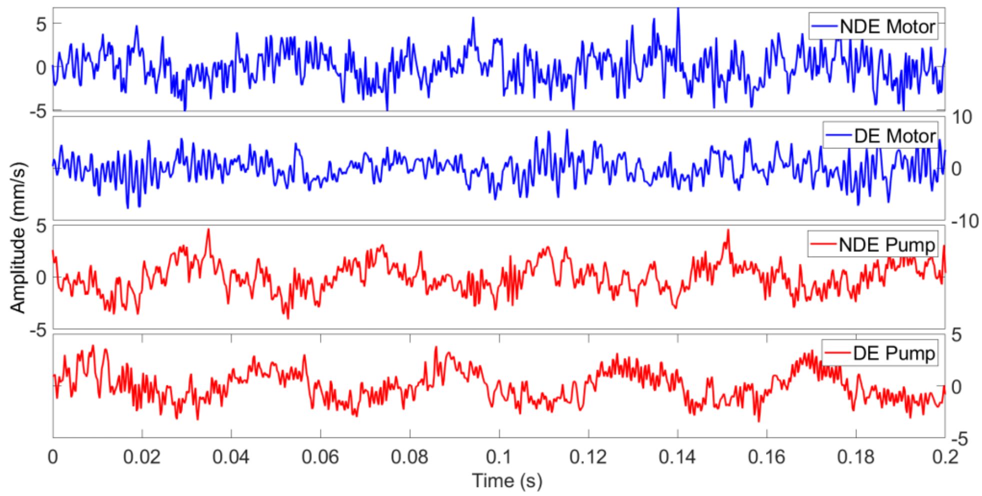


Figure 15. Time Domain After Repair

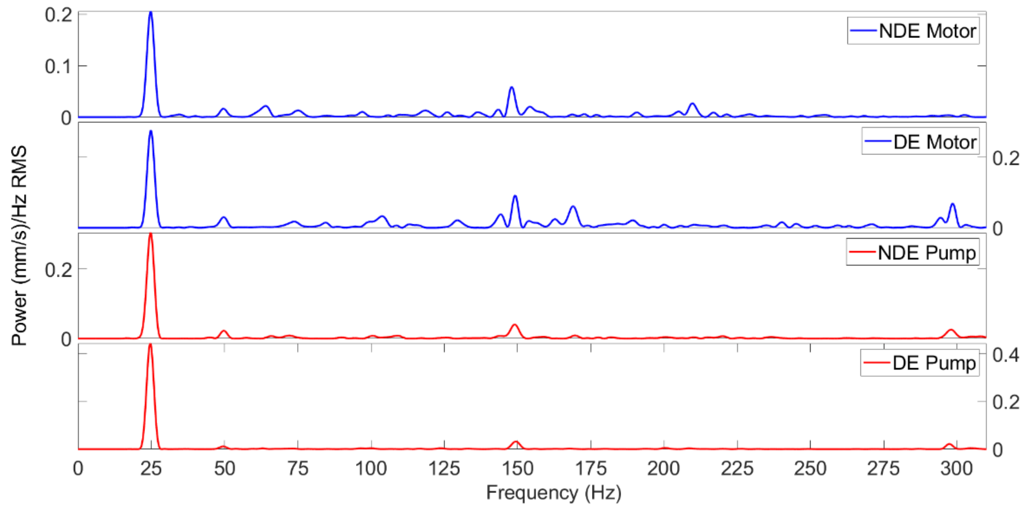


Figure 16. Overall PSD After Repair

## CONCLUSION

The source of excessive vibration in the centrifugal pump can be accurately identified by analyzing the vibration signal represented by the total RMS speed vibration value. The status of a centrifugal pump can be assessed by comparing its total RMS speed vibration value with the ISO 10816-3 standard. Based on the analysis results, the overall RMS vibration value decreased after the pump was repaired. The DE pump operates at a speed of 5.16 mm/s, indicating danger. The vibration value of the centrifugal pump decreased to 1.78 mm/s after repairs were carried out until it reached a satisfactory condition.

The FIR bandpass filter and Welch methods were successfully applied to decompose and transform centrifugal pump vibration signals. The advantage of using the Welch method is that the amplitude value in the spectrum will not change even if the applied frequency sample number setting is different. Besides that, it reduces low amplitude vibrations so that the spectrum looks smoother and contains only the main frequency components. Decomposing vibration signals using the FIR bandpass filter into frequency groups makes finding the dominant vibration source easier. Diagnostic findings include high vibrations at 1X, 2X, and BPF, which indicate misalignment and damage to the impeller. After repairs were performed based on frequency domain analysis, the vibration value decreased significantly.

## ACKNOWLEDGMENT

The authors express their heartfelt gratitude to Universitas Mercu Buana for its financial assistance under contract No. 02-5/33/B-SPK/II/2024.

## REFERENCES

[1] G. Yu, C. Wang, and Q. Zhang, “Numerical simulation of a high specific speed centrifugal pump,” *2022 5th World Conference on Mechanical Engineering and Intelligent Manufacturing, WCMEIM 2022*, 2022, pp.

188–191, doi: 10.1109/WCMEIM56910. 2022.10021451.

[2] B. A. Saputra and Nurato, “Performance analysis of a single-cylinder type steam turbine with a capacity of 3.5 MW using enthalpy drop method,” *SINERGI*, vol. 27, no. 3, pp. 319–326, Sep. 2023, doi: 10.22441/SINERGI.2023.3.003.

[3] S. Tampubolon, H. H. Purba, and C. Jaqin, “Flood Pump Performance Improvement Analysis Using DMAIC Method,” *AIP Conf Proc*, Dec. 2023, vol. 2680, no. 1, doi: 10.1063/5.0175389/2928404.

[4] R. Han, P. Li, and Z. Shi, “Implementation strategy of predictive maintenance in nuclear power plant,” *Proceedings - 2022 Prognostics and Health Management Conference, PHM-London 2022*, 2022, pp. 143–146, doi: 10.1109/PHM2022-LONDON52454.2022.00033.

[5] W. Prommachan, M. Pipathattakul, P. Surin, and P. Srinoi, “Predictive Maintenance Model for Rotating Machinery Using a Fuzzy Logic,” *2022 International Conference on Power, Energy and Innovations, ICPEI 2022*, 2022, doi: 10.1109/ICPEI55293.2022.9987151.

[6] C. Nata, Laurence, N. Hartono, and L. Cahyadi, “Implementation of Condition-based and Predictive-based Maintenance using Vibration Analysis,” *Proceedings - 2021 4th International Conference on Computer and Informatics Engineering: IT-Based Digital Industrial Innovation for the Welfare of Society, IC2IE 2021*, 2021, pp. 90–95, doi: 10.1109/IC2IE53219.2021.9649400.

[7] E. Babu, J. Francis, E. Thomas, R. Cherian, and S. S. Sunandhan, “Predictive Analysis of Induction Motor using Current, Vibration and Acoustic Signals,” *2022 2nd International Conference on Power Electronics and IoT Applications in Renewable Energy and its Control, PARC 2022*, 2022, doi: 10.1109/PARC52418.2022.9726688.

[8] F. Dreier, P. Günther, T. Pfister, J. W. Czarske, and A. Fischer, “Interferometric sensor system for blade vibration measurements in turbomachine applications,” *IEEE Transactions on Instrumentation and Measurement*, vol. 62, no. 8, pp. 2297–2302, 2013, doi: 10.1109/TIM.2013.2255993.

[9] Y. Zhang, W. Xu, Z. Li, and J. He, “Review of the vibration isolation technology of submarine thrust bearing,” *ICAC 2019 - 2019 25th IEEE International Conference on Automation and Computing*, Sep. 2019, doi: 10.23919/ICONAC.2019.8894976.

[10] J. Wang, L. Chen, Y. Wang, and L. Wei, “Vibration analysis and fault diagnosis of coupling misalignment,” *Proceedings - 2020 5th International Conference on Mechanical, Control and Computer Engineering, ICMCCE 2020*, Dec. 2020, pp. 452–455, doi: 10.1109/ICMCCE51767.2020.00105.

[11] J. Z. Wu, H. Long, X. L. Shi, L. Y. Ying, Z. W. Zheng, and B. P. Zhang, “Reduction of Lasing Threshold of GaN-Based Vertical-Cavity Surface-Emitting Lasers by Using Short Cavity Lengths,” *IEEE Trans Electron Devices*, vol. 65, no. 6, pp. 2504–2508, Jun. 2018, doi: 10.1109/TED.2018.2825992.

[12] N. Nicusor, L. Baicu, and B. Dumitrascu, “Vibration spectrum analysis using FFT in the microcontroller,” *2022 IEEE 28th International Symposium for Design and Technology in Electronic Packaging, SIITME 2022 - Conference Proceedings*, 2022, pp. 176–180, doi: 10.1109/SIITME56728.2022. 9987820.

[13] D. Bhaumik, A. Sadda, and G. S. Punekar, “Vibration signal analysis of induction motor bearing faults: Some aspects,” *International Conference on Smart Systems for Applications in Electrical Sciences, ICSSES 2023*, 2023, doi: 10.1109/ICSSES58299. 2023.10200270.

[14] X. Zhu, Y. Zhou, L. Zhang, Z. Peng, and W. Dong, “A fault detection and compensation strategy of the resolver for variable leakage flux permanent magnet motor with threshold self-regulation,” *IEEE J. Emerg. Sel. Top Power Electron*, vol. 12, no. 3, pp. 3063–3075, Jun. 2024, doi: 10.1109/JESTPE.2024.3382678.

[15] Y. Wang, L. Zheng, Y. Gao, and S. Li, “Vibration Signal Extraction Based on FFT and Least Square Method,” *IEEE Access*, vol. 8, pp. 224092–224107, 2020, doi: 10.1109/ACCESS.2020.3044149.

[16] X. Luo, H. Wang, T. Han, and Y. Zhang, “FFT-Trans: Enhancing robustness in mechanical fault diagnosis with Fourier Transform-Based Transformer under noisy conditions,” *IEEE Transactions on Instrumentation and Measurement*, vol. 73, pp. 1–12, 2024, doi: 10.1109/TIM.2024.3381688.

[17] L. Kämmerer, D. Potts, and T. Volkmer, “High-dimensional sparse FFT based on sampling along multiple rank-1 lattices,” *Appl Comput Harmon Anal*, vol. 51, pp. 225–257, Mar. 2021, doi: 10.1016/J.ACHA. 2020.11.002.

[18] J. Lian, X. Yang, and H. Wang, “Propagation characteristics analysis of high-frequency

vibration in pumped storage power station based on a 1D fluid-solid coupling model," *Journal of Energy Storage*, vol. 68, p. 107869, Sep. 2023, doi: 10.1016/J.EST.2023.107869.
[19] J. Taghipour, M. Dardel, and M. H. Pashaei, "Nonlinear vibration analysis of a flexible rotor shaft with a longitudinally dispositioned unbalanced rigid disc," *Commun Nonlinear Sci Numer Simul*, vol. 97, p. 105761, Jun. 2021, doi: 10.1016/J.CNSNS.2021.105761.
[20] M. H. Mohd Ghazali and W. Rahiman, "Vibration Analysis for Machine Monitoring and Diagnosis: A Systematic Review," *Shock and Vibration*, vol. 2021, no. 1, p. 9469318, Jan. 2021, doi: 10.1155/2021/9469318.
[21] D. J. Jwo, W. Y. Chang, and I. H. Wu, "Windowing Techniques, the Welch Method for Improvement of Power Spectrum Estimation," *Computers, Materials & Continua*, vol. 67, no. 3, pp. 3983–4003, Mar. 2021, doi: 10.32604/CMC.2021.014752.
[22] L. C. Astfalck, A. M. Sykulski, and E. J. Cripps, "*Debiasing Welch's Method for Spectral Density Estimation*," *Biometrika*, vol. 111, no. 4, pp. 1313–1329, December 2024, doi: 10.1093/biomet/asae033
[23] H. Ahmadi and Z. Khaksar, "Power Spectral Density Technique for Fault Diagnosis of an Electromotor," *Communications in Computer and Information Science*, vol. 165, pp. 105–112, 2011, doi: 10.1007/978-3-642-22247-4_9.
[24] D. Tang, F. Bi, J. Lin, X. Li, X. Yang, and X. Bi, "Adaptive recursive variational mode decomposition for multiple engine faults detection," *IEEE Transactions on Instrumentation and Measurement*, vol. 71, 2022, doi: 10.1109/TIM.2022.3173646.
[25] J. Chen et al., "A novel knowledge sharing method for rolling bearing fault detection against impact of different signal sampling frequencies," *IEEE Transactions on Instrumentation and Measurement*, vol. 72, 2023, doi: 10.1109/TIM.2023.3265088.
[26] R. R. Shubita, A. S. Alsadeh, and I. M. Khater, "Fault Detection in Rotating Machinery Based on Sound Signal Using Edge Machine Learning," *IEEE Access*, vol. 11, pp. 6665–6672, 2023, doi: 10.1109/ACCESS.2023.3237074.
[27] D. Romahadi, A. A. Luthfie, and L. B. D. Dorion, "Detecting classifier-coal mill damage using a signal vibration analysis," *SINERGI*, vol. 23, no. 3, pp. 175–183, Sep. 2019, doi: 10.22441/sinergi.2019.3.001.
[28] E. T. Bahtiar, N. Nugroho, D. Hermawan, W. Wirawan, and Khuschandra, "Triangle bracing system to reduce the vibration level of cooling tower – case study in PT Star Energy Geothermal (Wayang Windu) Ltd – Indonesia," *Case Studies in Construction Materials*, vol. 8, pp. 248–257, Jun. 2018, doi: 10.1016/J.CSCM.2018.01.006.
[29] J. Gorji, S. Pavan, and J. M. D. La Rosa, "On the use of fir feedback in bandpass delta-sigma modulators," *IEEE Transactions on Circuits and Systems I: Regular Papers*, vol. 71, no. 3, pp. 1082–1092, Mar. 2024, doi: 10.1109/TCSI.2023.3336719.
[30] A. S. Siva, S. G. Rameshkumar, and K. Dhayalini, "Supraharmonic Analysis by Welch's-Power Spectral Density Estimation," *2024 3rd International Conference on Power, Control and Computing Technologies, ICPC2T 2024*, pp. 357–362, 2024, doi: 10.1109/ICPC2T60072.2024.10474764.
[31] B. Eristi, "Classification of Power Quality Disturbances Using Welch-Based Power Spectral Density Features," *32nd IEEE Conference on Signal Processing and Communications Applications, SIU 2024 - Proceedings*, 2024, doi: 10.1109/SIU61531.2024.10600836.
[32] D. Romahadi, A. G. Feleke, and R. P. Youlia, "Evaluation of Laplacian Spatial Filter Implementation in Detecting Driver Vigilance Using Linear Classifier," *International Journal of Technology*, vol. 15, no. 6, pp. 1712–1729, 2024, doi: 10.14716/ijtech.V15I6.7166.
[33] S. C. Hsia and C. Y. Hsu, "Real-Time Monitor and Control System for Abnormal Motor Vibrations," *IEEE Transactions on Instrumentation and Measurement*, vol. 73, pp. 1–11, 2024, doi: 10.1109/TIM.2023.3331405.
[34] D. Romahadi et al., "Development of a smart system for gasoline car emissions diagnosis using Bayesian Network," *SINERGI*, vol. 27, no. 2, pp. 211-218, 2023, doi: 10.22441/sinergi.2023.2.009
[35] C. Yi, H. Wang, Q. Zhou, Q. Hu, P. Zhou, and J. Lin, "An Adaptive Harmonic Product Spectrum for Rotating Machinery Fault Diagnosis," *IEEE Transactions on Instrumentation and Measurement*, vol. 72, 2023, doi: 10.1109/TIM.2022.3230462.
[36] G. Zhu, F. Liu, X. Liu, S. Kumar, and X. Zhou, "Noise performance analysis and optimization of down sampling heterodyne Φ-OTDR," *IEEE Sensors Journal*, vol. 24, no. 9, pp. 14093–14100, May 2024, doi: 10.1109/JSEN.2024.3368227.